universität innsbruck

Bachelor thesis

Cumulant expansion of cavity sub- and superradiance

Sophia Simon

July 12, 2024

Supervised by Christoph Hotter, PhD
and Univ.-Prof. Mag. Dr. Helmut Ritsch
Institute for Theoretical Physics

Contents

1 Introduction **1**

2 Basic concepts **2**
2.1 Open quantum systems 2
2.2 Master equation 3
2.3 Cumulant expansion 5
2.4 The QuantumCumulants.jl framework 7
2.4.1 Usage 7
2.4.2 Symbolic indices and summations 10

3 The model **12**
3.1 Setup 12
3.2 Hamiltonian and Liouvillian 13

4 Simulation of the dynamics **15**
4.1 Results 15
4.2 Subradiance and superradiance 18

5 Conclusion **20**

Statutory declaration **21**

1 Introduction

The study of open quantum systems has recently attracted considerable attention due to its crucial role in understanding the behaviour of quantum systems interacting with their environments. Unlike closed systems, which are isolated from external influences, open quantum systems exchange energy and information with their environment. This exchange leads to many phenomena being central in modern quantum technologies such as quantum information processing or quantum communication which rely on the understanding of quantum states and their dynamics.

The ability of describing the time evolution of open quantum systems accurately is fundamental. The master equation provides a fundamental description of the time evolution of the density matrix in these systems and is therefore a powerful tool to model the dissipative processes of such systems. However, solving the master equation for large systems with many constituents remains a challenging task due to the exponential growth of the Hilbert space with the number of constituents.

To address this complexity, various approximation techniques have been developed. One such method is the cumulant expansion approach, which truncates higher-order quantum correlations, thereby simplifying the dynamics while retaining essential physical characteristics. This approach is particularly useful for studying systems with many particles where exact solutions are computationally infeasible.

In this thesis, we focus on a specific model of an open quantum system, where N two-level atoms are coupled to a single-mode cavity with alternating coupling. We employ the QuantumCumulants.jl framework, a computational tool based on the cumulant expansion approach, to simulate and analyse the dynamics of this system. The framework is well-suited for handling large open quantum systems and allows us to demonstrate the phenomena of cavity sub- and superradiance for this system.

2 Basic concepts

The purpose of this chapter is to introduce the fundamental theoretical concepts underlying the physical results of this thesis. We begin by explaining the concept of open quantum systems and continue with the introduction of the master equation. Then, we discuss the cumulant expansion as an approach to derive a numerical approximation for the time evolution of the system. Finally, we present the QuantumCumulants.jl framework, which utilizes the cumulant expansion.

2.1 Open quantum systems

The time evolution of a state vector $|\Psi(t)\rangle$ in a closed quantum system follows the Schrödinger equation:

$$i\hbar\frac{d}{dt}|\Psi(t)\rangle = H|\Psi(t)\rangle. \tag{2.1}$$

However, real-world systems interact with their environment, necessitating the description of such systems as open quantum systems. A prime example is a laser, where photons escape the cavity. In essence, an open quantum system comprises a system S coupled to its environment B, representing another larger quantum system. Typically, it is assumed that the combined system S+B is closed. The state of subsystem S evolves not only due to its internal dynamics but also owing to interactions with its surroundings. Figure 2.1 schematically depicts the system S and its environment B. The Hilbert space of the total system is described by the tensor product $\mathcal{H} = \mathcal{H}_\mathcal{S} \otimes \mathcal{H}_\mathcal{B}$, where $\mathcal{H}_\mathcal{S}$ represents the Hilbert space of the reduced system S, and $\mathcal{H}_\mathcal{B}$ denotes the Hilbert space of the environment B. The environment B is alternatively referred to as a reservoir if it possesses an infinite number of degrees of freedom. Moreover, the environment is termed a bath or heat bath when it is a reservoir in a thermal equilibrium state. The Hamiltonian of the combined system S+B can be expressed as

$$H(t) = H_S \otimes I_B + I_S \otimes H_B + \hat{H}_{\text{int}}(t) \tag{2.2}$$

where H_S and H_B denote the Hamiltonians of the systems S and B and $\hat{H}_{\text{int}}(t)$ denotes the Hamiltonian of the interaction of the two systems [1].

Solving the Schrödinger equation for the closed quantum system S+B , the coupled setup of the system and the environment, is excessively intricate and usually unnecessary, since we are only interested in the dynamics of the subsystem S, the open quantum system. To describe such an open quantum system, the master equation is introduced in the following section.

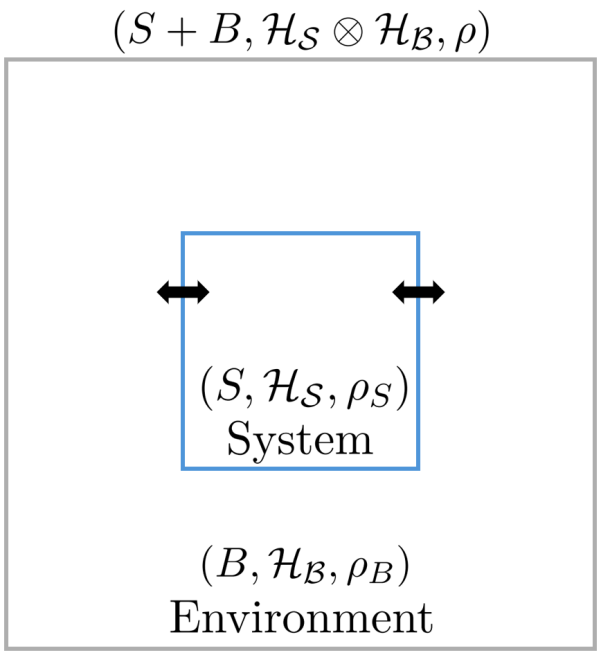

Figure 2.1: Schematic picture of an open quantum system S. With $\mathcal{H}_s$ the Hilbert space and ρ_s the density matrix of the system. In analogy $\mathcal{H}_B$ and ρ_B are the Hilbert space and the density matrix of the environment.

2.2 Master equation

Since we are only interested in the time evolution of the subsystem S, which constitutes an open quantum system, energy conservation is no longer assured. Consequently, there exists no Schrödinger equation describing the dynamics of the subsystem. The von Neumann equation is now employed to characterize the Quantum System S+B:

$$\frac{d\rho_{SB}}{dt} = \frac{i}{\hbar}[\rho_{SB}, H] \tag{2.3}$$

where ρ_{SB} denotes the density matrix. Conceptually, the density matrix assumes the role of the state vector $|\Psi\rangle$ and encapsulates all information concerning a quantum mechanical system.

The density matrix can be expressed as

$$\rho = \sum_\alpha \omega_\alpha |\Psi_\alpha\rangle\langle\Psi_\alpha| \tag{2.4}$$

where the $|\Psi_\alpha\rangle$ are normalized state vectors akin to those in the Schrödinger equation 2.1 and ω_α are their positive weights. Consequently, the density matrix can depict the system being in a mixed state [2]. Equation 2.3 can be easily derived by considering that the states $|\Psi_\alpha\rangle$ satisfy the Schrödinger equation. Hence, differentiating ρ using the product rule and utilizing the Schrödinger equation for the derivatives of the states $|\Psi_\alpha\rangle$ yields the von Neumann equation [1]. To obtain an equation solely describing the open subsystem, we need to perform the partial trace

over the environment in the von Neumann equation. To introduce the concept of the trace over a matrix, let's examine the expectation value of an observable for a mixed state, which can be expressed as

$$\langle A\rangle_\rho = \sum_\alpha \omega_\alpha \langle \Psi_\alpha | A | \Psi_\alpha \rangle \tag{2.5}$$

This expression can also be written using the trace of a matrix:

$$\begin{aligned} Tr(\rho A) &= Tr\left(\sum_\alpha \omega_\alpha |\Psi_\alpha\rangle\langle\Psi_\alpha| A\right) \\ &= \sum_n \sum_\alpha \omega_\alpha \langle n|\Psi_\alpha\rangle\langle\Psi_\alpha|A|n\rangle \\ &= \sum_\alpha \omega_\alpha \langle\Psi_\alpha| A \sum_n |n\rangle\langle n|\Psi_\alpha\rangle \\ &= \sum_\alpha \omega_\alpha \langle\Psi_\alpha|A|\Psi_\alpha\rangle \end{aligned} \tag{2.6}$$

utilizing the definition of the trace

$$Tr(D) := \sum_n \langle n|D|n\rangle. \tag{2.7}$$

Due to the definition of matrix multiplication, it's evident that $Tr(AB) = Tr(BA)$. By substituting, for example, B with the product BC, the invariance under cyclic permutation becomes apparent, hence [2]

$$\mathrm{Tr}(ABC) = \mathrm{Tr}(BCA) = \mathrm{Tr}(CAB). \tag{2.8}$$

Our objective now is to derive an equation describing the dynamics of the subsystem, known as the master equation. To obtain the density matrix of system S, we employ the partial trace operation [1]

$$\rho_S = tr_B\{\rho_{SB}\}. \tag{2.9}$$

Applying this operation to the von Neumann equation yields

$$\frac{d\rho_S}{dt} = \frac{i}{\hbar} tr_B[\rho_{SB}, H]. \tag{2.10}$$

Therefore we have now derived an equation of motion for the reduced denstiy matrix ρ_s. The dynamics of the reduced system S, defined by the exact equation 2.10 are quite involved. Therefore two assumptions are now taken. Firstly, we assume that the interaction between the system and the environment is absent at $t = 0$. Secondly, we assume that the interaction between the system and the environment does not alter the state of the environment. Consequently, we can express the density matrix as $\rho_{SB} = \rho_S \otimes \rho_B$, known as the Born-Markov approximation. As a result, there is no back-action of the system on itself, as the influence of the system on the environment is neglected. Applying these assumptions enables the derivation of the master equation, which describes the dynamics of the system S, as demonstrated in [1].

The resulting equation is

$$\frac{d}{dt}\rho_S = -i[H, \rho_S] + \mathcal{L}[\rho_S] \tag{2.11}$$

with the density matrix ρ_S the Hamiltonian H and the Liouvillian super-operator $\mathcal{L}$. It is important to notice, that H is not always equal to the Hamiltonian H_S of the reduced system, since H may contain additional terms which are due to the coupling of the system to its environment [1]. The Liouvillian $\mathcal{L}$ characterises dissipative processes such as atomic or cavity decay and can be expressed in the standard Lindblad form as:

$$\mathcal{L}[\rho_S] = \frac{1}{2}\sum_j R_j(2J_j\rho J_j^\dagger - J_j^\dagger J_j\rho - \rho J_j^\dagger J_j) \tag{2.12}$$

under consideration of the Born-Markov approximation [3]. Here J_j are the jump operators describing the dissipative processes of the system. For instance, in the case of a laser, these operators would delineate phenomena such as cavity photon loss, decay of atoms coupled to the cavity and dephasing of atoms. Meanwhile, R_j denotes the rates associated with these processes, such as the rate of photons leaving the cavity, the decay rate, and the dephasing rate of the atoms. A more detailed description of a single atom laser is given in section 2.4.1.

In conclusion equation 2.11 describes the time evolution of an open quantum system S which is interacting with its environment B.

2.3 Cumulant expansion

The solution of the master equation would provide the full time evolution of the density matrix and since the density matrix is describing the complete quantum state of the system, the solution equals the full description of the open quantum system. However the master equation is usually not analytically solvable, therefore a numerical approach to solve the equation is needed. Another problem is that the size of the Hilbert space describing the system is growing exponentially with the constituents of the system. An example for this exponential growth is the description of the state of a system with N two-level atoms. The vector describing the state of the atoms is then of a size scaling as 2^N and the operators are of a size $2^N \times 2^N$. Therefore exact numerical solutions are limited to small systems and in order to treat configurations of higher numbers of subsystems a technique to reduce the problem size is needed. One approach is the cumulant expansion which is neglecting quantum correlations of higher order, this leads to a sufficiently accurate description of systems with low quantum correlations. This approach was initially introduced by R. Kubo [4].

Since one is often only interested in specific operator expectation values it is advantageous to look at the time evolution of those operator expectation values. An equation for the time derivative of an operator expectation value can be derived from the master equation 2.11. Assuming that the operators are not explicitly time dependent in the Heisenberg picture, the time derivative of an operator can be expressed as

$$\frac{d}{dt}\langle\mathcal{O}\rangle = tr\{\mathcal{O}\rho\} = tr\{\mathcal{O}\frac{d}{dt}\rho\}. \tag{2.13}$$

Inserting the master equation 2.11 and the Liouvillian 2.12 we obtain

$$\frac{d}{dt}\langle\mathcal{O}\rangle = -itr\{\mathcal{O}[H,\rho]\} + \frac{1}{2}\sum_j R_j(2tr\{\mathcal{O}J_j\rho J_j^\dagger\} - tr\{\mathcal{O}J_j^\dagger J_j\rho\} - tr\{\mathcal{O}\rho J_j^\dagger J_j\}) \tag{2.14}$$

Using the cyclic permutation property of the trace it follows [3]

$$\frac{d}{dt}\langle\mathcal{O}\rangle = -i\langle[H,\mathcal{O}]\rangle + \frac{1}{2}\sum_j R_j(2\langle J_j^\dagger\mathcal{O}J_j\rangle - \langle\mathcal{O}J_j^\dagger J_j\rangle - \langle J_j^\dagger J_j\mathcal{O}\rangle). \tag{2.15}$$

We now encounter the problem that equation 2.15 depends on other expectation values of operators and operator products. In order to find the solution of the operator $\mathcal{O}$ we would need a closed set of coupled differential equations to calculate all appearing expectation values. Therefore we would also need to derive the time derivatives of all appearing operator products. Those derivatives of operators then consequently depend again on operator products of higher order for which again the equations of motion need to be derived to find a closed set of differential equations. Doing this procedure to its end would be equal to solving the full master equation. Our goal is to find a good approximation for the solutions of the time evolution of the operators we are interested in via the cumulant expansion. In order to introduce the assumption which is made with the approach of the cumulant expansion we need to investigate the quantum correlation of a product of operators. A measure of the quantum correlation in a product of n operators is the joint cumulant

$$\langle\mathcal{O}_1\mathcal{O}_2...\mathcal{O}_n\rangle_c = \sum_{p\in P(\mathcal{I})}(|p|-1)!(-1)^{|p|-1}\prod_{B\in p}\langle\prod_{i\in B}\mathcal{O}_i\rangle \tag{2.16}$$

with $\mathcal{I} = \{1,2,...n\}$, $\mathcal{P}(\mathcal{I})$ the set of all partitions of $\mathcal{I}$, $|p|$ denotes the length of the partition p, and B runs over the blocks of each partition [3]. The joint cumulant represents the difference between the average of order n and lower orders. A vanishing joint cumulant indicates, that at least one operator in the product is independent of the others. Looking at the equation 2.16 we see that if the joint cumulant vanishes we can write the product of the average of n operators as an expression of only n-1 and lower order products. As an example we take two Operators $\mathcal{O}_1$ and $\mathcal{O}_2$ with a vanishing joint cumulant. Equation 2.16 gives us the expression for the joint cumulant

$$\langle\mathcal{O}_1\mathcal{O}_2\rangle_c = \langle\mathcal{O}_1\mathcal{O}_2\rangle - \langle\mathcal{O}_1\rangle\langle\mathcal{O}_2\rangle \tag{2.17}$$

Due to the absence of quantum correlations between $\mathcal{O}_1$ and $\mathcal{O}_2$ 2.17 simplifies to

$$\langle\mathcal{O}_1\mathcal{O}_2\rangle = \langle\mathcal{O}_1\rangle\langle\mathcal{O}_2\rangle. \tag{2.18}$$

In general the average value for a product of n operators with at least one independent operator can be expressed as [3]

$$\langle\mathcal{O}_1\mathcal{O}_2...\mathcal{O}_n\rangle = \sum_{p\in P(\mathcal{I})\setminus\mathcal{I}}(|p|^{-1})!(-1)^{|p|}\prod_{B\in p}\langle\prod_{i\in B}\mathcal{O}_i\rangle. \tag{2.19}$$

Equation 2.19 is exact if the joint cumulant of the operator product is zero, otherwise it yields an approximation. The cumulant expansion is assuming that the joint cumulant of an operator product is zero and is therefore neglecting quantum correlations in case of operator products with no independent operator. Equation 2.19 yields the cumulant expansion of (n-1)-th order for a vanishing joint cumulant. An example for the second order cumulant expansion is:

$$\langle\mathcal{O}_1\mathcal{O}_2\mathcal{O}_3\rangle \longrightarrow \langle\mathcal{O}_1\mathcal{O}_2\rangle\langle\mathcal{O}_3\rangle - \langle\mathcal{O}_1\rangle\langle\mathcal{O}_2\mathcal{O}_3\rangle - \langle\mathcal{O}_1\mathcal{O}_3\rangle\langle\mathcal{O}_2\rangle + 2\langle\mathcal{O}_1\rangle\langle\mathcal{O}_2\rangle\langle\mathcal{O}_3\rangle. \tag{2.20}$$

Keeping products to the n-th order is called the n-th order cumulant expansion. To make the procedure of the cumulant expansion more clear we take a closer look at the equations of motion of a single-atom laser as an example. This example is explained in more detail in the section 2.4.1. We use the equation 2.15 to derive the time evolution of the operators a, $\dot{\sigma}^{ge}$ and $\dot{\sigma}^{ee}$. Calculating the commutators and products of the operators and averaging over the resulting equations yields

$$\langle \dot{a} \rangle = -(i\Delta + \frac{\kappa}{2})\langle a \rangle - ig\langle \sigma^{ge} \rangle \tag{2.21a}$$

$$\langle \dot{\sigma}^{ge} \rangle = -\frac{\gamma + \nu}{2}\langle \sigma^{ge} \rangle + ig\langle a\sigma^{ee} \rangle \tag{2.21b}$$

$$\langle \dot{\sigma}^{ee} \rangle = -\gamma\langle \sigma^{ee} \rangle + \nu(1 - \langle \sigma^{ee} \rangle) + ig(\langle a^\dagger \sigma^{ge} \rangle - \langle a\sigma^{eg} \rangle) \tag{2.21c}$$

[5]. Looking at the averaged equations 2.21 operator products appear on the right hand side. To obtain a closed system of coupled differential equations the cumulant expansion of first order is now applied to the operator products. This leads to

$$\langle \dot{a} \rangle = -(i\Delta + \frac{\kappa}{2})\langle a \rangle - ig\langle \sigma^{ge} \rangle \tag{2.22a}$$

$$\langle \dot{\sigma}^{ge} \rangle = -\frac{\gamma + \nu}{2}\langle \sigma^{ge} \rangle + ig\langle a \rangle\langle \sigma^{ee} \rangle \tag{2.22b}$$

$$\langle \dot{\sigma}^{ee} \rangle = -\gamma\langle \sigma^{ee} \rangle + \nu(1 - \langle \sigma^{ee} \rangle) + ig(\langle a^\dagger \rangle\langle \sigma^{ge} \rangle - \langle a \rangle\langle \sigma^{eg} \rangle). \tag{2.22c}$$

These equations now are a closed set of equations which is solvable. In conclusion the cumulant expansion approach is neglecting quantum correlations of operator products and therefore makes it possible to describe larger quantum systems since the number of equations is only scaling as N^n for the n-th order cumulant expansion of a system with N constituents [3].

2.4 The QuantumCumulants.jl framework

This section demonstrates the usage of the QuantumCumulants.jl framework with the example of a single atom laser. Additionally, it introduces the extension of symbolic indices and summation.

2.4.1 Usage

The QuantumCumulants.jl framework is written in the Julia programming language and is based on the cumulant expansion approach. It is able to automatically derive the equations of motion for operator averages in the Heisenberg picture. Consequently the framework enables the user to simulate large open quantum systems. This section provides a brief overview of the fundamental workflow when using the framework. We will describe the usage of the framework with a well known example, the simplest quantum model of a laser. In this model a two-level atom is placed inside an optical cavity as depicted in 2.2. The dynamics of this system are described by the Jaynes-Cummings Hamiltonian, expressed as

$$H_{JC} = \hbar g(a^\dagger \sigma^{ge} + a\sigma^{eg}), \tag{2.23}$$

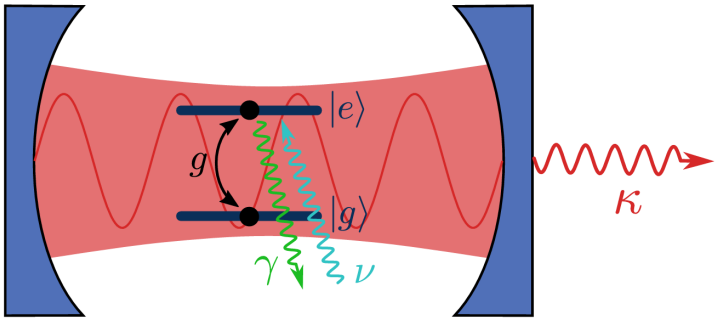

Figure 2.2: Schematic picture of a single atom laser. The frequency g is the coupling between the cavity and the atom. $|g\rangle$ is the ground state of the atom and $|e\rangle$ the excited state. The atom can spontaneously emit a photon at a rate γ and is also incoherently driven from the ground to the excited state at a rate ν . The cavity is losing photons at a rate κ. Figure from [5].

in the absence of detuning between the cavity resonance frequency and the atomic transition frequency [5]. Here, g represents the coupling strength between the cavity and the atom. The transition operators σ^{ge} and σ^{eg} describe the atomic transitions between the ground state $|g\rangle$ and the excited state $|e\rangle$. The atom spontaneously emits photons at a rate γ, represented by the jump operator σ^{ge}, and is also incoherently driven from the ground state to the excited state at a rate ν, described by the jump operator σ^{eg}. The photonic annihilation operator a accounts for cavity photon loss at a rate κ.

To address a problem using the mentioned framework, one must first define the Hilbert space. The Hilbert spaces we use here are the `FockSpace` and the `NLevelSpace`. The `FockSpace` describes the quantum harmonic oscillator, while the `NLevelSpace` represents a finite set of discrete energy levels. An example of the `NLevelSpace`'s usage is the description of multi-level atoms. The framework implements operators as non-commutative variables defined on Hilbert spaces. Therefore, as explained in Section 2.1, the Hilbert spaces of the subsystems need to be defined first. The complete Hilbert space is then determined by the tensor product of the subsystem Hilbert spaces. Operators must be defined on the complete Hilbert space to perform algebraic combinations of operators. We can now proceed by defining the Hilbert space for the single atom laser that has already been introduced.

```
using QuantumCumulants

h_cav = FockSpace(:cavity)
h_atom = NLevelSpace(:atom, (:g,:e))
h = h_cav ⊗ h_atom
```

In the first line the framework is imported. Then, the Hilbert space of the cavity is defined as `h_cav` using the `FockSpace`, in the next line the Hilbert Space of the atom is defined as `h_atom` using the `NLevelSpace`. Finally the tensor product of both Hilbert spaces defines the entire Hilbert space `h`.

The next step is defining the fundamental operators and the parameters. Using these, the

Hamiltonian of the system can be defined, as demonstrated in the following code sample.

```
@cnumbers κ γ ν g
@qnumbers a::Destroy(h) σ::Transition(h)

H = g*(a'*σ(:g,:e) + a*σ(:e,:g))
J = [a,σ(:g,:e),σ(:e,:g)]
rates = [κ, γ, ν]
```

All variables are defined using the `@cnumbers` annotation, while the operators are defined using the `@qnumbers` annotation and their corresponding callable functions acting on the total Hilbert space `h`. We can now use these operators and variables to define the Hamiltonian `H`, which in this case is the Jaynes-Cummings Hamiltonian without detuning, as introduced earlier. Next, the dissipative processes are specified. The array `J` contains the jump operators representing the decay processes of the system. The array `rates` then defines the corresponding rate for each dissipative process.

The framework can now derive the equations of motion for a set of operators, demonstrated here for the single atom laser in the following code sample:

```
eqs = meanfield([a, σ(:g,:e), σ(:e,:e)], H, J; rates=rates, order=2)
eqs_completed = complete(eqs)
```

When invoking the `meanfield` function, equations of motion are derived for the specified operators in the first argument. The last argument of the function determines the order of operator products retained in these equations, corresponding to the order of the cumulant expansion employed. These equations are referred to as n-th order meanfield equations, with n denoting the chosen order in the `meanfield` function. Here, we derive the second-order meanfield equations.

Subsequently, the equations are finalized by invoking the `complete` function. In our case, the output of the `complete` function leads to the following closed set of equations:

$$\partial_t(\langle a\rangle) = (0-1im)\cdot g\cdot\langle\sigma^{ge}\rangle - 0.5\langle a\rangle\cdot\kappa$$

$$\partial_t(\langle\sigma^{ge}\rangle) = (0+2im)\cdot g\cdot\langle a\cdot\sigma^{ee}\rangle + (0-1im)\cdot g\cdot\langle a\rangle - 0.5\langle\sigma^{ge}\rangle\cdot(\gamma+\nu)$$

$$\partial_t(\langle\sigma^{ee}\rangle) = \nu + (0-1im)\cdot g\cdot\langle a\cdot\sigma^{eg}\rangle + (0+1im)\cdot g\cdot\langle a^\dagger\cdot\sigma^{ge}\rangle + \langle\sigma^{ee}\rangle\cdot(-\gamma-\nu)$$

$$\begin{aligned}\partial_t(\langle a\sigma^{ee}\rangle) = {}& \langle a\cdot\sigma^{ee}\rangle\cdot(-\gamma-\nu) - 0.5\langle a\cdot\sigma^{ee}\rangle\cdot\kappa + \langle a\rangle\cdot\nu \\ & + (0+1im)\cdot g\cdot(\langle a\sigma^{ge}\rangle\cdot\langle a^\dagger\rangle + \langle a^\dagger\sigma^{ge}\rangle\cdot\langle a\rangle + \langle\sigma^{ge}\rangle\cdot\langle a^\dagger\cdot a\rangle - 2\langle a^\dagger\rangle\langle a\rangle\cdot\langle\sigma^{ge}\rangle) \\ & + (0-1im)\cdot g\cdot(2\langle a\cdot\sigma^{eg}\rangle\cdot\langle a\rangle + \langle a\cdot a\rangle\cdot\langle\sigma^{eg} - 2(\langle a\rangle^2)\cdot\langle\sigma^{eg}\rangle)\end{aligned}$$

$$\begin{aligned}\partial_t(\langle a\sigma^{eg}\rangle) = {}& (0-1im)\cdot g\cdot\langle\sigma^{ee}\rangle + (0+1im)\cdot g\cdot\langle a^\dagger a\rangle \\ & - 0.5\langle a\cdot\sigma^{eg}\rangle\cdot(\gamma+\kappa+\nu) \\ & + (0-2im)\cdot g\cdot(\langle\sigma^{ee}\rangle\cdot\langle a^\dagger a\rangle + \langle a^\dagger\rangle\cdot\langle a\cdot\sigma^{ee}\rangle \\ & + \langle a\rangle\cdot\langle a^\dagger\sigma^{ee}\rangle - 2\langle\sigma^{ee}\rangle\cdot\langle a^\dagger\rangle\cdot\langle a\rangle)\end{aligned}$$

$$\begin{aligned}\partial_t(\langle a\sigma^{ge}\rangle) = &(0-1im)\cdot g\cdot\langle a\cdot a\rangle - 0.5\langle a\cdot\sigma^{ge}\rangle\cdot(\gamma+\kappa+\nu)\\ &+(0+2im)\cdot g\cdot(\langle\sigma^{ee}\rangle\cdot\langle a\cdot a\rangle + 2\langle a\sigma^{ee}\rangle\cdot\langle a\rangle\\ &-2\langle\sigma^{ee}\rangle\cdot(\langle a\rangle^2))\end{aligned}$$

$$\partial_t(\langle a^\dagger a\rangle) = (0+1im)\cdot g\cdot\langle a\cdot\sigma^{eg}\rangle + (0-1im)\cdot g\cdot\langle a^\dagger\sigma^{ge}\rangle - \langle a^\dagger\cdot a\rangle\cdot\kappa$$

$$\partial_t(\langle a\cdot a\rangle) = (0-2im)\cdot g\cdot\langle a\sigma^{ge}\rangle - \langle a\cdot a\rangle\cdot\kappa$$

With an increasing number of atoms in the cavity, the number of equations grows rapidly, leading to a corresponding increase in computational complexity. A recent update to QuantumCumulants.jl addresses this issue by leveraging specific symmetries to simplify both the equations and the computational workload. This extension introduces symbolic indices and summations, which are further discussed in the next section [6].

2.4.2 Symbolic indices and summations

In this chapter, the usage of indices and summations in QuantumCumulants.jl is introduced. An index is a named object that includes the entire Hilbert space, a specified range, and the Hilbert space of the subsystem on which the index operates [6]. The following code sample demonstrates an exemplary definition of an index:

```
@cnumbers N

#Hilbert space
h1 = FockSpace(:cavity)
h2 = NLevelSpace(:atom,2)
h = h1 ⊗ h2

k = Index(h,:k,N,2)
```

In the example, we defined a complete Hilbert space `h` composed of two individual Hilbert spaces, `h1` and `h2`. An index named `k` is then defined on the Hilbert space `h`, specifying that it acts on the second Hilbert space `h2`. The upper limit of the index is `N`, which is defined as a c-number using the `@cnumbers` macro. Now, we can utilize these `Index` objects in combination with operators to define `IndexedOperators`. The definition of an `IndexedOperator` looks like this:

```
σ(α,β,k) = IndexedOperator(Transition(h, :σ, α, β, 2),k)
```

Here the transition operator σ is defined with the index `k`. Additionally, it is possible to perform summations over this defined index, as illustrated in the following example of defining a Hamiltonian.

```
H =
 Ω*0.5*∑((σ1(2,1,i)+σ1(1,2,i)),i) +
 Ω*0.5*∑((σ2(2,1,j)+σ2(1,2,j)),j) +
 g1*∑(( a'*σ1(1,2,i) + a*σ1(2,1,i) ),i) +
```

```
g2*∑(( a'*σ2(1,2,j) + a*σ2(2,1,j) ),j)
```

Here the summation over the indices `i` and `j` is performed. The extension is utilized in the following to simulate the model which is introduced in the next chapter.

3 The model

The purpose of this chapter is to explain the model of the system that will be simulated using the QuantumCumulants.jl framework in the subsequent chapter. First, we present the setup and components of the system. Next, we discuss the Hamiltonian that describes the system's dynamics. Finally, the mean-field equations of the system are presented.

3.1 Setup

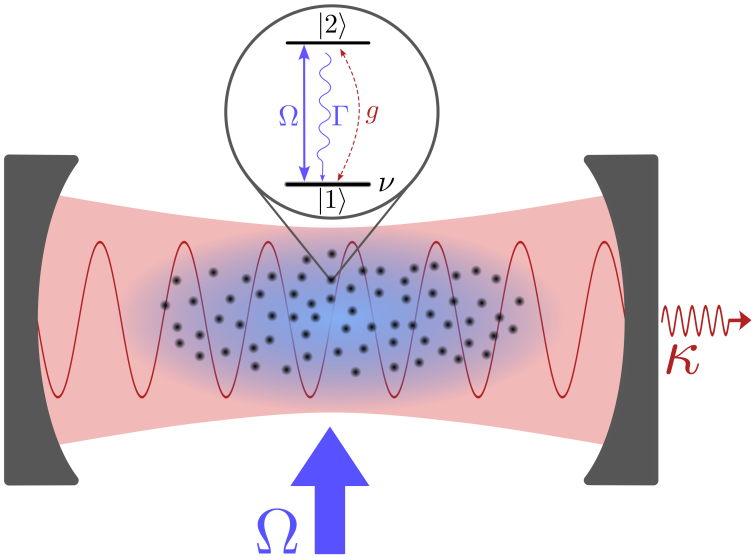

Figure 3.1: Cavity Sub- and Superradiance Model. A dilute, homogeneous ensemble of two-level atoms at random but fixed positions coupled to a standing wave optical resonator is depicted. The ensemble is coherently driven by a transverse plane wave laser with a frequency Ω. Each atom is coupled to the cavity mode with a coupling $g_j = (-1)^j g$ with alternating signs. Every atom j has a ground state $|1\rangle_j$ and an excited state $|2\rangle_j$, the atomic decay rate is Γ. The cavity photon loss rate is κ and the dephasing rate is ν.

The system that we simulate consists of a dilute, homogeneous ensemble of two-level atoms at random but fixed positions coupled to a standing wave optical resonator, where each atom j has a ground state $|1\rangle_j$ and an excited state $|2\rangle_j$. The ensemble is coherently driven by a transverse plane wave laser with a frequency Ω. We assume that there is no detuning between the laser and the atomic transition, as it is shown in Figure 3.1. The system includes a damped cavity mode, along with atomic decay and dephasing, described by the cavity photon loss rate κ, the atomic

decay rate Γ and the dephasing rate ν. Furthermore, we assume a weak single atom coupling but a strong collective regime, i.e.,

$$\kappa,\ \sum_j \frac{g_j^2}{\kappa} \gg \Gamma \gg g_j^2/\kappa \tag{3.1}$$

[7]. This regime implies a very large atom number, making a full quantum simulation of the model impractical. However, we can effectively address this problem using a second-order cumulant expansion, which will be detailed in the following chapter.

Another assumption we make to describe this model is that the atoms are located close to the cavity mode antinodes, with half of the atoms at the maxima and the other half at the minima of the mode function along the cavity axis. Due to this assumption, their coupling can be approximated by $g_j = (-1)^j g$.

3.2 Hamiltonian and Liouvillian

In order to simulate the dynamics of the system the Hamiltonian of the system is required. Therefore we first need to define the operators appearing in this Hamiltonian. We defined the states of the N two level atoms as $|1\rangle_j$ and $|2\rangle_j$. The atomic transition operator is generally defined as

$$\sigma^{kl} = |k\rangle\langle l| \tag{3.2}$$

hence we identify the two atomic transition operators σ^{12} and σ^{21} for the two level atoms, where σ^{12} represents a transition from the excited state to the ground state and σ^{21} a transition from the ground state to the excited state [7]. The products of atomic transition operators are computed as [5]

$$\sigma^{ij}\sigma^{kl} = \delta_{jk}\sigma^{il}. \tag{3.3}$$

Consequently, the product either gives another atomic transition operator or vanishes. In the context of the cavity field, the photon creation operator $a^\dagger$ and the photon annihilation operator a are used. They are defined as

$$a^\dagger|n\rangle = \sqrt{n+1}|n+1\rangle \tag{3.4}$$

and

$$a|n\rangle = \sqrt{n}|n-1\rangle, \tag{3.5}$$

where $|n\rangle$ is an eigenstate of the number operator $\hat{n} = \hat{a}^\dagger\hat{a}$. Consequently, the relation $\hat{n}|n\rangle = n|n\rangle$ holds. Note that the explicit notation $\hat{\mathrm{O}}$ is used for operators to clearly distinguish them from their eigenvalues [8]. In the case of our cavity field n reflects the number of photons, consequently the creation operator increases the photon number by one and the annihilation operator decreases the photon number by one. The annihilation and creation operators satisfy the commutation relation [5]

$$[a, a^\dagger] = 1. \tag{3.6}$$

Therefore the product $aa^\dagger$ is equal to $a^\dagger a + 1$. The Hamiltonian of the system in the rotating frame of the pump laser is the Tavis-Cummings Hamiltonian with an additional drive term:

$$H = \sum_{j=1}^{N} g_j(\sigma^{21}a + \sigma^{12}a^\dagger) + \sum_{j=1}^{N} \frac{\Omega}{2}(\sigma_j^{21} + \sigma_j^{12}) \tag{3.7}$$

where g_j is the coupling rate of the j-th atom [7]. The described system is an open quantum system, consequently we also need to define all jump operators J_i and their corresponding rates R_i, since the Liouvillian in the master equation is describing the dissipative processes of the system. In Table 3.1 all decay processes with their jump operators and rates are listed.

i	J_i	R_i	Description
1	a	κ	cavity decay
2	σ_j^{12}	Γ	atomic decay
3	σ_j^{22}	ν	dephasing of the j-th atom

Table 3.1: Dissipative processes. The system includes a damped cavity mode, along with atomic decay and dephasing, described by the cavity photon loss rate κ, the atomic decay rate Γ and the dephasing rate ν.

Before simulating the system using the QuantumCumulants.jl framework with a second-order cumulant expansion, we present the mean-field equations for a qualitative description of the system.

The mean-field equations of the model 3.1 encapsulate the key physics of the system and can therefore be employed for a qualitative analysis. The equations are

$$\frac{d}{dt}\langle a\rangle = -\frac{\kappa}{2}\langle a\rangle - i\sum_{j=1}^{N} g_j\langle\sigma_j^{12}\rangle \tag{3.8a}$$

$$\frac{d}{dt}\langle\sigma_j^{22}\rangle = -\Gamma\langle\sigma_j^{22}\rangle + i\frac{\Omega}{2}[\langle\sigma_j^{12}\rangle - \langle\sigma_j^{21}\rangle] + ig_j[\langle a^\dagger\rangle\langle\sigma_j^{12}\rangle - \langle a\rangle\langle\sigma_j^{21}\rangle] \tag{3.8b}$$

$$\frac{d}{dt}\langle\sigma_j^{12}\rangle = -\frac{\Gamma+\nu}{2}\langle\sigma_j^{12}\rangle + i\left(\frac{\Omega}{2} + g_j\langle a\rangle\right)\left[2\langle\sigma_j^{22}\rangle - 1\right] \tag{3.8c}$$

These simplified equations already explain some of the behaviour of the model simulated in the next section. For instance the sum $\sum_{j=1}^{N} g_j\langle\sigma_j^{12}\rangle$ shows the significance of the alternating coupling, the summation indicates that the cumulative dipole moment of the atoms projected on the cavity mode only vanishes for alternating coupling [7]. In general the number of equations for a first order treatment is $1 + 2N$ and for a second order treatment it is $\frac{N(N-1)}{2} + 2N + 1$, where N is the number of subsystems and is equal to the number of atoms if we treat them individually. Since all atoms start in the same state, we can assume that ($\langle\sigma_1^{22}\rangle = \langle\sigma_3^{22}\rangle = ...$) and ($\langle\sigma_2^{22}\rangle = \langle\sigma_4^{22}\rangle = ...$). Due to the alternating coupling, the model consists of two non-identical subsystems and we obtain five mean field equations and six equations for a second order treatment. This approach drastically reduces the number of equations and allows us to study systems with large atomic numbers [3].

4 Simulation of the dynamics

In this section, we simulate the dynamics of the model previously described using the QuantumCumulants.jl framework. We begin by examining the superradiant behaviour of an inverted ensemble and then demonstrate the subradiant behaviour of a non-inverted ensemble. Finally, we quantitatively describe the phenomena.

4.1 Results

The parameters that were used for this simulation are $N = 2 \cdot 10^5$, $\kappa = 10^3\,\Gamma$, $\Omega = 10^4\,\Gamma$, $\nu = 10\,\Gamma$ and the coupling is $g_1 = 10\,\Gamma$ for half of the atoms of the ensemble and $g_2 = -10\,\Gamma$ for the other half. For the chosen parameters the relation 3.1 holds:

$$\kappa \gg \Gamma \gg \frac{g_j^2}{\kappa} \qquad \Longleftrightarrow \qquad 10^3\,\Gamma \gg \Gamma \gg 0.1\,\Gamma \tag{4.1a}$$

$$\sum_j \frac{g_j^2}{\kappa} \gg \Gamma \qquad \Longleftrightarrow \qquad 2 \cdot 10^4\,\Gamma \gg \Gamma \tag{4.1b}$$

First, we consider an inverted ensemble. An ensemble is inverted if more than 50% of the atoms are excited. Here, we prepare it such that initially 100% of the atoms are excited. The average of the operator σ^{22} corresponds to the probability of an atom being excited, hence $\langle \sigma^{22} \rangle = 1$ initially. To achieve this, the atoms are inverted with a fast π-pulse, meaning they are coherently driven by the laser for a time $t = \frac{\pi}{\Omega}$. If the pulse duration is shorter than that, the atoms will be less excited, resulting in a lower inversion, wich is much faster than any other time scale of the system.

The time evolution of the operators $\langle \sigma^{22} \rangle$ and $\langle a^\dagger a \rangle$ is depicted in Figure 4.1. Figure 4.1 a) shows the time evolution of $\langle \sigma^{22} \rangle$, starting at 1.0 after the preparation. Initially, the inversion remains relatively constant, followed by a rapid decrease of the excited state population. This decrease is caused by cavity-enhanced superradiant decay, where synchronized emission in the cavity is stimulated [7]. Figure 4.1 b) illustrates the time evolution of $\langle a^\dagger a \rangle$ for the inverted ensemble. Initially, there are no photons in the cavity. After a certain time, the photon number increases, reaching its peak value. Subsequently, the intracavity photon number decreases back to zero. The initial increase in photon number is a result of superradiant decay of the atoms in the cavity. Photons leave the cavity at a rate κ, and since the atoms are only initially driven for a time $t = \frac{\pi}{\Omega}$, the photon number decreases again, eventually leading to the emission of a delayed intense light pulse.

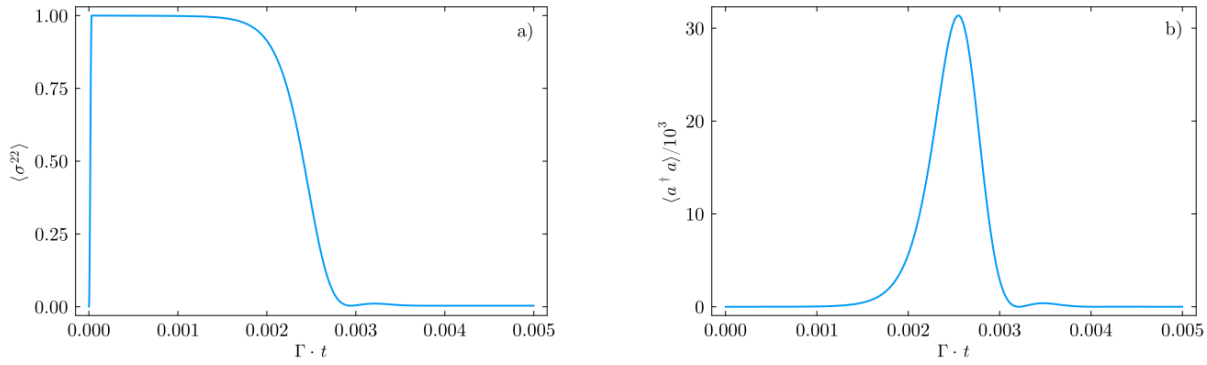

Figure 4.1: Time evolution of the operators $\langle \sigma^{22} \rangle$ and $\langle a^\dagger a \rangle$ for an inverted ensemble. Figure a) shows the time evolution of $\langle \sigma_{22} \rangle$ for an inverted ensemble. The atoms are prepared at $\langle \sigma_{22} \rangle = 1$. The inversion of the ensemble decreases after time due to cavity-enhanced superradiant decay [7]. Figure b) shows the time evolution of the intracavity photon number. We see a time delayed increase of the photon number in the cavity due to the cavity-enhanced superradiant decay of the inverted ensemble. Next, the intracavity number decreases again due to photons leaving the cavity. A delayed intense light pulse is emitted.

Next, we examine a non-inverted ensemble, where initially the atoms are less than 50% excited. This condition requires the pulsing time t to be shorter than $\frac{\pi}{2\Omega}$. Figure 4.2 illustrates the time evolution of the average operator $\langle \sigma^{22} \rangle$ and the intracavity photon number $\langle a^\dagger a \rangle$ for a pulsing time $t = \frac{\pi}{3\Omega}$, corresponding to a non-inverted ensemble. In Figure 4.2 a), we observe the evolution of $\langle \sigma^{22} \rangle$. Initially, the atoms are prepared with $\langle \sigma^{22} \rangle \approx 25\%$. The inversion of the atoms remains nearly constant over time. Comparing this with the time evolution of the intracavity photon number depicted in Figure 4.2 b), we observe that not a significant amount of photons is emitted into the cavity. Consequently, in this scenario, superradiant emission is strongly suppressed due to the lack of initial inversion, characteristic of subradiant behavior [7].

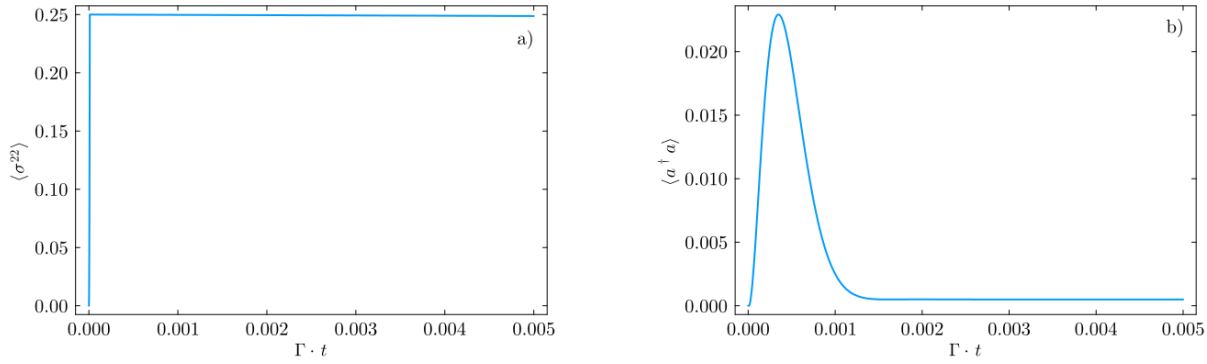

Figure 4.2: Time evolution of the operators $\langle \sigma^{22} \rangle$ and $\langle a^\dagger a \rangle$ for an non inverted ensemble. Figure a) shows the time evolution of the excited state population $\langle \sigma^{22} \rangle$. The ensemble is prepared at $\langle \sigma^{22} \rangle \approx 25\%$. $\langle \sigma^{22} \rangle$ is nearly constant over time. Figure b) shows the time evolution of the intracavity photon number $\langle a^\dagger a \rangle$. The maximum value of $\langle a^\dagger a \rangle$ is below 0.03 meaning that not a significant amount of photons is emitted in the cavity. The ensemble features subradiant behaviour.

The behaviour of the ensemble depends on its initial inversion $\langle\sigma^{22}\rangle$. Consequently, the number of photons leaving the cavity over time also depends on this inversion. Figure 4.3 illustrates the total number of emitted photons $\langle a^\dagger a\rangle_{out} = \kappa \int \langle a^\dagger a\rangle dt$ per atom as a function of the ensemble's inversion. The plot shows two regimes, the subradiant regime for initial $\langle\sigma^{22}\rangle < 0.5$ and the superradiant regime for $\langle\sigma^{22}\rangle > 0.5$. For the subradiant regime the plot shows that the total number of emitted photons is almost zero since not a significant amount of photons are emitted in the cavity and superradiant emission is strongly suppressed. In contrast, the superradiant regime $\langle a^\dagger a\rangle_{out}/N$ increases linearly with $\langle\sigma^{22}\rangle$. When $\langle\sigma^{22}\rangle = 1$, each atom emits a photon into the cavity.

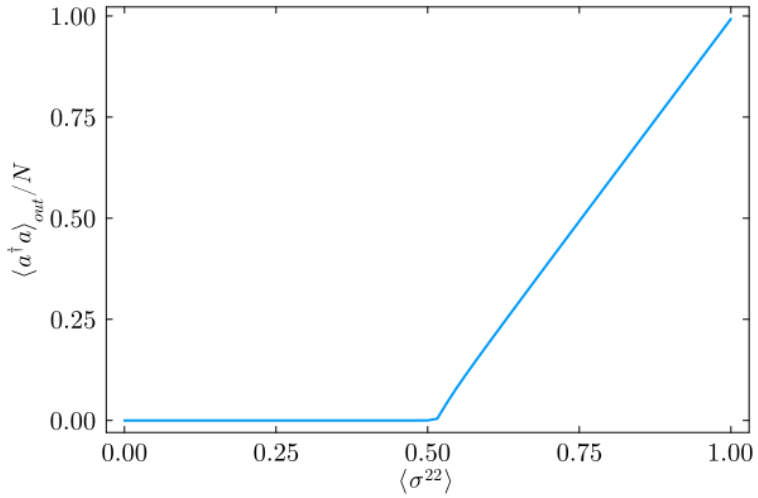

Figure 4.3: Cavity-output photon number $\langle a^\dagger a\rangle_{out} = \kappa \int \langle a^\dagger a\rangle dt/N$ as a function of the excited state population $\langle\sigma^{22}\rangle$ of the ensemble . The subradiant regime for $\langle\sigma^{22}\rangle < 0.5$, the superradiant regime for $\langle\sigma^{22}\rangle > 0.5$.

In the next section the superradiant regime is described quantitatively.

4.2 Subradiance and superradiance

In this section, we quantitatively describe the phenomena of subradiance and superradiance. Our approach focuses on examining the scaling of the emitted peak photon number for different numbers of atoms. To observe superradiance, we initially prepare an inverted ensemble and analyze the time evolution of the intracavity photon number. In Figure 4.4, the time evolution of $\langle a^\dagger a \rangle$ is depicted for an inverted ensemble with $N = 2 \cdot 10^4$ atoms (blue curve) and $N = 4 \cdot 10^4$ atoms (orange curve). For an inverted ensemble, the peak photon number in the cavity scales proportionally to the square of the number of atoms [7].

In the case depicted in Figure 4.4, the proportionality of peak photon numbers to the square of the number of atoms does not apply perfectly for several reasons. Firstly, there are multiple peaks in both graphs, with the highest peak having a lower photon number. The smaller peaks arise because some photons do not leave the cavity directly; instead, they are reflected at the cavity mirrors and may re-excite atoms. Secondly, the scaling with N^2 occurs for atoms coupled to the same bath or in the bad-cavity limit. In the case where multiple peaks are observed for each graph in Figure 4.4, the back action of photons on the atoms is evident. This scenario indicates that we are not in the bad-cavity limit, where exact scaling of the peak photon number cannot be demonstrated perfectly.

Nevertheless, it can be demonstrated that the peak photon number scales more than linearly with the number of atoms coupled to the cavity mode. This contrasts with the typically expected exponential decay observed for independent atoms due to spontaneous emission. Additionally, a time delay of the emitted light pulse is generally observed. Figure 4.4 illustrates that the time delay decreases as the number of atoms increases.

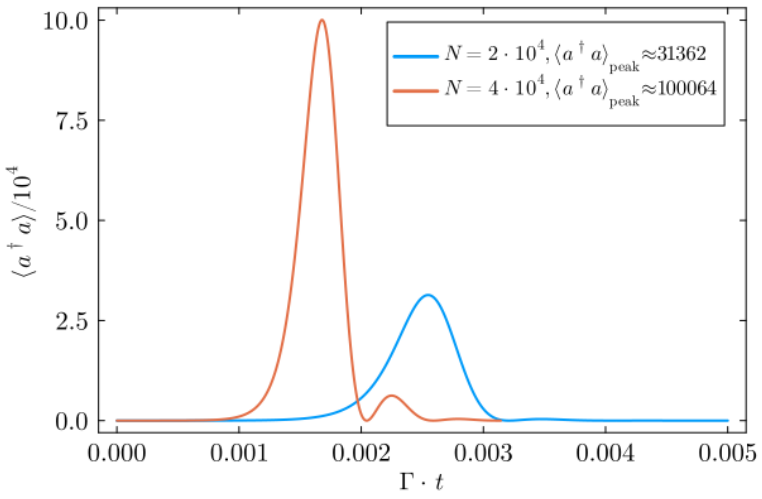

Figure 4.4: Time evolution of the intracavity photon number $\langle a^\dagger a \rangle$ for two inverted ensembles with different atom numbers. In blue an atom number of $N = 2 \cdot 10^4$ is coupled to the cavity. The peak intracavity photon number is $\langle a^\dagger a \rangle_{peak} = 31362$ for this ensemble. In comparison the orange graph shows an ensemble with twice as many atoms coupled to the cavity, the resulting peak intracavity photon number is $\langle a^\dagger a \rangle_{peak} = 100064$.

In Figure 4.5, the time evolution of $\langle a^\dagger a \rangle$ is depicted for a non-inverted ensemble with $N = 2{\cdot}10^4$ atoms (blue curve) and an inverted ensemble with $N = 4 \cdot 10^4$ atoms (orange curve). The peak photon number for the non-inverted ensemble is orders of magnitude smaller than that for the inverted ensemble, and it scales less than linearly with the number of atoms N coupled to the cavity mode.

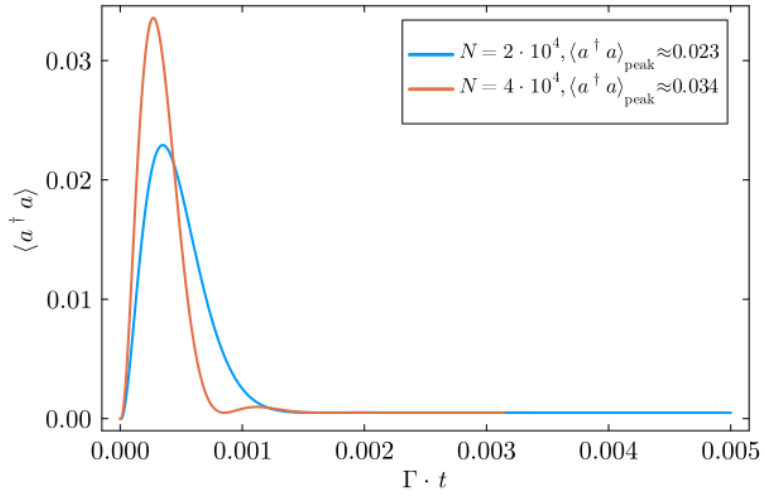

Figure 4.5: Time evolution of the intracavity photon number $\langle a^\dagger a \rangle$ for two non inverted ensembles with different atom numbers. In orange an atom number of $N = 2 \cdot 10^4$ is coupled to the cavity. The peak intracavity photon number is $\langle a^\dagger a \rangle_{peak} \approx 0.023$ for this ensemble. In comparison the blue graph shows an ensemble with twice as many photons coupled to the cavity, the resulting peak intracavity photon number is $\langle a^\dagger a \rangle_{peak} \approx 0.034$.

5 Conclusion

This thesis has examined the dynamics of open quantum systems, focusing on a model with N two-level atoms coupled to a single mode cavity. By leveraging the QuantumCumulants.jl framework we have effectively simulated the system's behaviour.

We began by explaining the basic concepts necessary for understanding the dynamics of open quantum systems. This included an introduction of the master equation, which provides a fundamental description of the time evolution of the density matrix in these systems. We then discussed the cumulant expansion approach, which allows for the approximation of complex quantum dynamics by truncating higher-order quantum correlations. The QuantumCumulants.jl framework was introduced as a powerful tool for the simulation of large open quantum systems, since it is based on the cumulant expansion approach.

In the modeling section, we described the setup of our specific system, a model of N two-level atoms coupled to a single mode cavity with alternating coupling. The Tavis-Cummings Hamiltonian was introduced as the Hamiltonian of the system and the Liouvillian was derived describing the systems dissipative processes. This provided the necessary foundation for simulating the system's dynamics.

Through simulations, we analysed the behaviour of the system for inverted ensembles and non inverted ensembles. For an inverted ensemble we have demonstrated cavity-enhanced superradiant decay and for a non inverted ensemble we have demonstrated the strong supression of the superradiant emission. Therefore the separation in the subradiant regime for $\langle \sigma^{22} \rangle < 0.5$ and the superradiant regime for $\langle \sigma^{22} \rangle > 0.5$ was demonstrated.

This behaviour was already experimentally confirmed, as shown in [9]. This paper additionally demonstrates how to take advantage of the sub- to superradiant transition that was demonstrated in this thesis, highlighting practical applications of this transition.

In conclusion, this thesis has provided a comprehensive study of the dynamics of a single mode cavity with coupled two-level atoms, demonstrating the phenomena of sub- and superradiance with the use of the QuantumCumulants.jl framework.

Statutory declaration

I hereby declare in lieu of an oath with my own handwritten signature that I have written this thesis independently and have not used any sources or aids other than those specified. All passages that have been taken from the specified sources, either verbatim or in terms of content, are marked as such.
I agree to the archiving of this bachelor thesis.

Innsbruck, on July 12, 2024 Sophia Simon

Bibliography

[1] H.-P. Breuer und F. Petruccione, *The theory of open quantum systems*, OUP Oxford (2002).

[2] D. T. Haar, *Theory and applications of the density matrix*, Reports on Progress in Physics, **24**(1), 304 (1961).

[3] C. Hotter, *Collective Quantum Dynamics for Large Ensembles of Clock Atoms in Optical Cavities* (2023).

[4] R. Kubo, *Generalized cumulant expansion method*, Journal of the Physical Society of Japan, **17**(7), 1100 (1962).

[5] D. Plankensteiner, C. Hotter und H. Ritsch, *QuantumCumulants.jl: A Julia framework for generalized mean-field equations in open quantum systems*, Quantum, **6**, 617 (2022).

[6] J. Moser, *Symbolic Indices and Summations in QuantumCumulants. jl.*

[7] C. Hotter, L. Ostermann und H. Ritsch, *Cavity sub- and superradiance for transversely driven atomic ensembles*, Phys. Rev. Res., **5**, 013056 (2023).

[8] F. Schwabl, *Quantenmechanik (QMI)*, Springer-Verlag (2013).

[9] E. A. Bohr, S. L. Kristensen, C. Hotter, S. A. Schäffer, J. Robinson-Tait, J. W. Thomsen, T. Zelevinsky, H. Ritsch und J. H. Müller, *Collectively enhanced Ramsey readout by cavity sub-to superradiant transition*, Nature Communications, **15**(1), 1084 (2024).